LETTERS

Modifications to the edge current profile with auxiliary edge current drive and improved confinement in a reversed-field pinch

B. E. Chapman,[a)] T. M. Biewer, P. K. Chattopadhyay, C.-S. Chiang, D. J. Craig,
N. A. Crocker, D. J. Den Hartog, G. Fiksel, P. W. Fontana,[b)] S. C. Prager, and J. S. Sarff
Department of Physics, University of Wisconsin-Madison, Madison, Wisconsin 53706

Auxiliary edge current drive is routinely applied in the Madison Symmetric Torus [R. N. Dexter, D. W. Kerst, T. W. Lovell *et al.*, Fusion Technol. **19**, 131 (1991)] with the goal of modifying the parallel current profile to reduce current-driven magnetic fluctuations and the associated particle and energy transport. Provided by an inductive electric field, the current drive successfully reduces fluctuations and transport. First-time measurements of the modified edge current profile reveal that, relative to discharges without auxiliary current drive, the edge current density decreases. This decrease is explicable in terms of newly measured reductions in the dynamo (fluctuation-based) electric field and the electrical conductivity. Induced by the current drive, these two changes to the edge plasma play as much of a role in determining the resultant edge current profile as does the current drive itself. © *2000 American Institute of Physics.* [S1070-664X(00)04109-4]

The reversed-field pinch is a toroidal magnetically confined plasma. Its principal distinguishing feature is its toroidal magnetic field, whose direction in the plasma edge is reversed relative to its direction in the core. Reversed-field pinch plasmas exhibit large-amplitude, internally resonant magnetic fluctuations which allow rapid radial transport of particles and energy. These fluctuations are driven primarily by the gradient in the current-density profile, and although they are locally resonant, the fluctuations are globally perturbative and are sensitive to the shape of the current profile over much of the plasma.

The current in the reversed-field pinch (RFP) is driven both by the applied toroidal electric field and the self-generated dynamo electric field. According to magnetohydrodynamics (MHD), the dynamo electric field arises from the correlated product of velocity and magnetic fluctuations (see, e.g., Ref. 1). In standard RFP discharges, the applied toroidal electric field constitutes antiparallel current drive in the region outside the toroidal magnetic field reversal radius, but parallel current is observed here. This current in the Madison Symmetric Torus (MST) (Ref. 2) has been shown to be driven by the MHD dynamo.[3–5]

For several years, auxiliary edge current drive has been applied to RFP plasmas with the goals of replacing the dynamo-driven current and modifying the parallel current profile to reduce current-driven instability. In the most successful current-drive technique, referred to as pulsed poloidal current drive, a poloidal (parallel) electric field is induced by transiently increasing the reversed toroidal magnetic flux in the edge.[6–9] In the MST RFP, this auxiliary current drive reduces magnetic and electrostatic fluctuations everywhere in the plasma.[10,11] Particle and energy transport have thereby been reduced (confinement has been improved) by at least a factor of five.[7,8] It was anticipated that if the auxiliary current drive successfully reduced fluctuations, the dynamo electric field would also be reduced. However, given the increased inductive parallel electric field, we could not predict the net response of the edge current. Knowledge of the resultant current profile is critical to understanding the means by which fluctuations are reduced in these discharges.

First-time measurements of the edge current profile during periods of reduced fluctuations with auxiliary current drive reveal that the edge current density is reduced (where, for purposes of this work, the edge is defined as the outer 15% of the plasma, in minor radius). The reduction is due primarily to the anticipated reduction in the dynamo electric field. However, the edge electron temperature also decreases, implying a reduction in the electrical conductivity (assuming no significant change in the mean ionic charge). Thus, the dynamo and conductivity reductions induced by the current
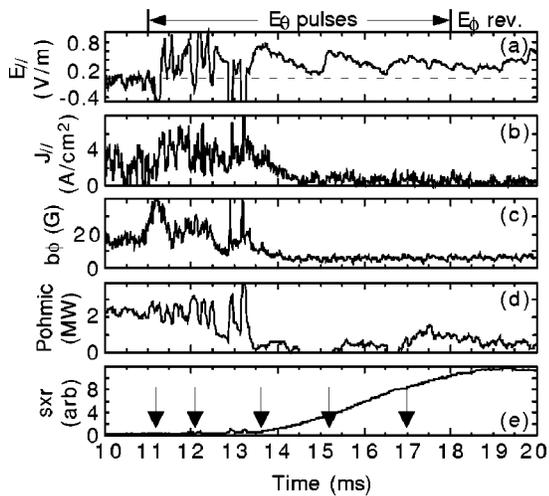
FIG. 1. In a discharge with auxiliary edge current drive and a period of improved confinement, (a) inductive parallel electric field at the plasma boundary, (b) parallel current 3 cm from the plasma boundary (48 cm minor radius), (c) rms fluctuation in the toroidal magnetic field, (d) estimated ohmic input power, and (e) soft x-ray intensity. Five poloidal electric field (E_θ) pulses, which peak at the times indicated by arrows at the bottom of the figure, are followed by toroidal electric field (E_ϕ) reversal.

drive play as much of a role in determining the resultant edge current profile as does the current drive itself.

The data described here were gathered in MST plasmas with toroidal plasma currents ranging from 150–200 kA and line-averaged electron densities ranging from $5–8 \times 10^{18} \, \text{m}^{-3}$. The ohmically heated MST plasma has major and minor radii of 150 and 51 cm, respectively. The primary diagnostics used in this work are probes which are inserted into the plasma edge. One of the probes is comprised of both a Rogowski coil, used to measure the local current density, and a set of magnetic sensing coils, used to measure the local fluctuating and equilibrium magnetic field. A triple Langmuir probe was used to measure the edge electron temperature. A new optical probe was employed to measure velocity fluctuations of ions in the plasma edge.[12] The probe essentially consists of two optical fibers which transmit light from the plasma edge to a Doppler spectrometer.[13] Each fiber's view has a radial and a toroidal component, and the fibers face in opposite toroidal directions. Plates mounted across from each fiber limit the collection of light to a region extending 5 cm radially and toroidally. We have measured the velocity fluctuations of singly-ionized helium ions radiating at 4685.7 Å. To collect sufficient radiation, we fueled the discharges with helium. The other data discussed in this Letter were gathered in similar hydrogen or deuterium discharges.

A discharge in which auxiliary current drive induces a period of reduced fluctuations, improved confinement, and reduced edge current density is shown in Fig. 1. The auxiliary current drive begins at 11 ms, while the period of fluctuation and edge-current reduction begins around 13.5 ms. Figure 1(a) contains the inductive parallel electric field at the plasma boundary, $E_\parallel \equiv \mathbf{E} \cdot \mathbf{B}/B = (E_\theta B_\theta + E_\phi B_\phi)/B$, which is small before the current drive begins. Here, B is the equilibrium magnetic field, and the subscripts θ and ϕ represent poloidal and toroidal directions, respectively. Normally, B_θ

$\gg B_\phi$ in the plasma edge. Thus, parallel current drive is most easily accomplished through an increase in E_θ, which is induced by transiently increasing the reversed toroidal flux in the plasma edge. The poloidal electric field is induced in a series of five triangular-shaped pulses, which peak at the times indicated by arrows at the bottom of Fig. 1. At about 18 ms, when the last E_θ pulse has decayed away, we reverse E_ϕ. By this time, the edge toroidal magnetic field has increased significantly, to about $B_\theta/2$, and reversal of E_ϕ yields a significant parallel electric field. This additional auxiliary current drive lengthens periods of reduced fluctuations. The first two $E_\parallel(E_\theta)$ pulses in Fig. 1 are largely obscured by brief electric field bursts, which are induced by bursts of plasma-generated toroidal flux and which will be described in more detail elsewhere. The bursts are also observed in the edge parallel current density, $J_\parallel \equiv \mathbf{J} \cdot \mathbf{B}/B$. Figure 1(b) contains $J_\parallel$ measured 3 cm from the plasma boundary.

After the bursts cease, the current decays almost to zero, showing relatively little response to the auxiliary electric field pulses. In otherwise similar discharges with the same auxiliary-electric-field amplitude and timing, the transition to reduced edge current occurs at different times and occasionally not at all. The reduction of edge current is accompanied by reduced fluctuations and improved confinement. The reduction of toroidal magnetic fluctuations is illustrated in Fig. 1(c). Previously, periods such as this lasted only about 3 ms,[7,8] but reversal of E_ϕ combined with longer and improved sustainment of E_θ (achieved by increasing the number of electric field stages and by firing the stages closer together in time) has lengthened them up to 10 ms.[14] The magnetic fluctuation reduction is accompanied by a reduction in the ohmic input power. A power-balance estimate of the ohmic power is shown in Fig. 1(d). While the decrease in the ohmic power is firmly established, the extent to which it decreases is not yet well-determined. The power-balance estimate depends on the time dependent magnetic stored energy, but the extreme changes to the magnetic field associated with improved electric field sustainment preclude accurate measurement of this quantity. This inaccuracy results in occasional zero values of the ohmic input power. In addition to the reduced ohmic input power, the plasma temperature increases, indicated qualitatively by the increasing soft x-ray emission in Fig. 1(e). In improved-confinement discharges similar to those described in this Letter, the total beta increases from 9% to 14%, due primarily to a large change in the on-axis electron temperature, which increases from 200 to 550 eV. At the same time, the energy confinement time increases from 1.4 to an estimated 9 ms.

The reduction of current density with auxiliary current drive, as well as a steepening of the current profile, occur over roughly the outer 15% of the plasma. Profiles of $J_\parallel$ measured during standard discharges and during periods of improved confinement with current drive are shown in Fig. 2(a). The corresponding profiles of $J_\parallel/B$, which determine the theoretical linear stability of current-driven magnetic fluctuations, are shown in Fig. 2(b). Each point in these profiles is an ensemble average of time-averaged data from several similar discharges. The standard data set excludes sawtooth crashes, which cause a transient increase in the edge
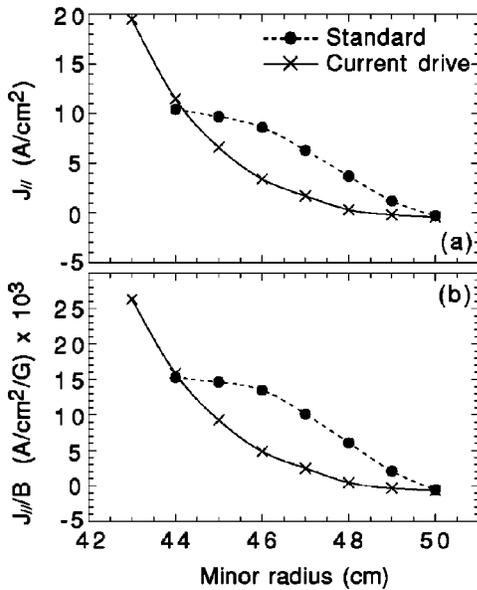
FIG. 2. From discharges with auxiliary current drive and improved confinement and from standard-confinement discharges, without auxiliary current drive, (a) parallel current density, and (b) parallel current density normalized to the local magnetic field. Plasma boundary is at 51 cm. Statistical error bars are same size as the plot symbols.

FIG. 3. The electron temperature, to the power of 3/2, ($\times$) from discharges with auxiliary current drive and current reduction and ($\bullet$) from standard-confinement discharges, without auxiliary current drive. The data at 39 cm are from Thomson scattering, while the other data are from the Langmuir probe. Inset is an expanded view of the probe data. Except for the error bar shown, statistical error bars are same size as the plot symbols. Plasma boundary is at 51 cm.

current,[3–5] and the improved-confinement data set excludes bursts, which sometimes appear during periods when the edge current is otherwise reduced. In the standard current profile, there is a flat region centered at 45 cm. Since the current profile must steepen further inside the plasma (the estimated current density at the plasma center is about 80 A/cm^2), this flat region is expected to be localized. The flattening may be due to the quasilinear effect of poloidal mode number $m=0$ fluctuations, which are resonant in the flattened region. With current drive, the increase in the reversed toroidal magnetic field moves the $m=0$ resonant surface deeper inside the plasma.

The reduction of edge parallel current is qualitatively explicable in terms of modifications to the terms in parallel Ohm's law, which can be cast as $J_\parallel = \sigma(E_\parallel + E_f)$, where $\sigma \propto T_e^{3/2}/Z$ is the electrical conductivity, T_e is the electron temperature, Z is the mean ionic charge, $E_\parallel$ is the applied parallel electric field, $E_f = \langle \mathbf{v} \times \mathbf{b} \rangle_\parallel$ is the fluctuation-induced parallel dynamo electric field, and $\mathbf{v}$ and $\mathbf{b}$ are the fluctuating velocity and magnetic field, respectively. In the edge of standard plasmas without current drive, $E_\parallel$ is small and negative, while it becomes larger and positive with auxiliary current drive. Thus, the reduction of current with auxiliary current drive must entail a decrease in σ and/or E_f.

To detect changes in σ, we measured the edge temperature with a Langmuir probe. We are as yet unable to measure Z. Profiles of $T_e^{3/2}$ are shown in Fig. 3. In each of the profiles, we have included data at 39 cm from our Thomson scattering diagnostic. Due to thermal loading of the Langmuir probe tips, which increases with insertion depth and can distort the data, we only insert the probe to a minor radius of 48 cm. All of the data points are averages over an ensemble of similar discharges. In the absence of current drive, the probe-measured edge temperature is roughly constant in time, but during periods of reduced fluctuations like that in Fig. 1, T_e

decreases with a time evolution similar to that of the edge current. This is concurrent with the large increase in the central electron temperature. Comparing the profiles of the probe-measured data (inset in Fig. 3), the temperature change in the current-drive case contributes to a reduction in the electrical conductivity of about a factor of two. Plasma–wall interaction and impurity influx decrease in the current-drive case, so we expect that Z will decrease in the edge. Hence, the net conductivity likely decreases modestly, at most by a factor of two.

The other term in Ohm's law that can contribute to the decrease in edge current is $E_f = \langle \mathbf{v} \times \mathbf{b} \rangle_\parallel \approx \langle v_\phi b_r - v_r b_\phi \rangle$, where the subscript r indicates the radial direction, and the brackets indicate a flux surface average. The optical probe, used to measure velocity fluctuations, is quite perturbative relative to the other probes used here. In discharges with auxiliary current drive, it extends by several ms the bursty phases like that in Fig. 1. Burst-free periods were only achievable by limiting the insertion of the optical and magnetic sensing probes to a minor radius of 48 cm. The probes were at the same toroidal location but separated by about 18° poloidally.

With auxiliary current drive, the two fluctuation products, $|v_\phi||b_r|$ and $|v_r||b_\phi|$, not including the cross-coherence or cross-phase, decrease substantially. This is illustrated in Fig. 4, in which we present the time evolutions of data averaged over 43 similar discharges. In all 43 discharges, the auxiliary current drive begins at 10.1 ms, and only discharges whose bursty phases end by 18 ms were included in the ensemble. In Fig. 4(a) is the inductive parallel electric field at the plasma boundary, in which one can discern the five poloidal electric field pulses followed by toroidal electric field reversal. The ohmic input power in Fig. 4(b) reaches a minimum from about 18–19 ms due to the cessation of the bursts. In the last two plots are the fluctuation products, which decrease rather suddenly at about 12.5 ms, reflecting a decrease in the frequency of the bursts. A further, albeit slight, decrease occurs after about 18 ms, when the bursts are finally suppressed altogether.

Including the coherence and phase, the total dynamo electric field in the burst-free period (from 18–19 ms) in Fig.
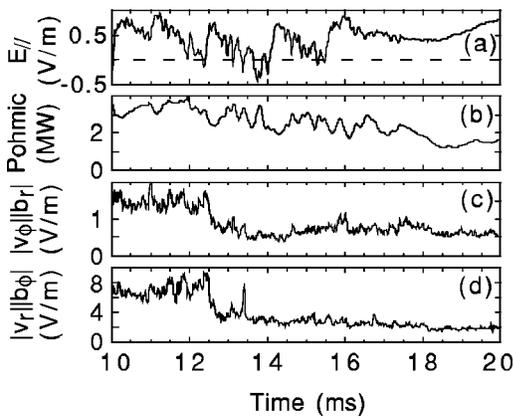
FIG. 4. From an ensemble of 43 similar discharges with current drive beginning at 10.1 ms (a) parallel electric field at the plasma boundary, (b) estimated ohmic input power, (c) and (d) products of velocity and magnetic fluctuations, not including coherence and phase, measured 3 cm from the plasma boundary (48 cm minor radius).

4 is about 0.16 V/m. Before 18 ms (before the randomly occurring bursts are suppressed), the coherence between the velocity and magnetic fluctuations is low, and the phase between these fluctuations is indeterminate. At the same minor radius in standard plasmas, E_f is about 0.83 V/m between sawtooth crashes, and it reaches about 9.2 V/m during crashes.[4,5] Thus, the dynamo electric field decreases by about a factor of five from its between-crash value in standard plasmas and by over a factor of 50 compared to its value during crashes.

In summary, we have shown that with auxiliary edge current drive and improved confinement, the edge current is reduced. The reduction occurs largely due to the reduction in the dynamo electric field, but also due to a probable decrease in the electrical conductivity. Recent work in standard discharges has shown that E_f in the plasma edge is due primarily to fluctuations associated with edge-resonant, poloidal mode number $m = 0$ fluctuations.[4,5] Thus, it is believed that the reduction of E_f described here is due primarily to the observed reduction of these fluctuations, described elsewhere. The reduced edge temperature and electrical conductivity must stem from the changes in heating and/or energy transport brought about by the auxiliary current drive, but determination of the relative importance of these changes will require transport analysis based on more detailed profile measurements.

In addition to the edge current reduction, the edge current profile steepens, and the shape of the resulting current profile (Fig. 2) matches fairly well the corresponding profile of $T_e^{3/2}$ (Fig. 3). Since $E_\parallel$ is roughly constant over the plasma edge (and assuming that Z is roughly constant as well), Ohm's law may be approximately satisfied without the dynamo electric field term, i.e., $J_\parallel \approx \sigma E_\parallel \propto (T_e^{3/2}/ZE_\parallel)$, over the entire edge plasma.

Reduction of edge current has also been observed in nonlinear MHD simulations in which auxiliary current drive led to reductions of fluctuations and the dynamo electric field.[15,16] However, further understanding of the role of current drive and the current profile in RFP confinement improvement requires measurement of the full current, pressure, and flow profiles and inclusion of these profiles in theory and computation.

ACKNOWLEDGMENTS

[1] S. Ortolani and D. D. Schnack, *Magnetohydrodynamics of Plasma Relaxation* (World Scientific, Singapore, 1993).

[2] R. N. Dexter, D. W. Kerst, T. W. Lovell, S. C. Prager, and J. C. Sprott, Fusion Technol. **19**, 131 (1991).

[3] H. Ji, A. F. Almagri, S. C. Prager, and J. S. Sarff, Phys. Rev. Lett. **73**, 668 (1994).

[4] P. W. Fontana, Ph.D. thesis, University of Wisconsin-Madison, Madison, 1999.

[5] P. W. Fontana, D. J. Den Hartog, G. Fiksel, and S. C. Prager, Phys. Rev. Lett. **85**, 566 (2000).

[6] J. S. Sarff, S. A. Hokin, H. Ji, S. C. Prager, and C. R. Sovinec, Phys. Rev. Lett. **72**, 3670 (1994).

[7] J. S. Sarff, N. E. Lanier, S. C. Prager, and M. R. Stoneking, Phys. Rev. Lett. **78**, 62 (1997).

[8] M. R. Stoneking, N. E. Lanier, S. C. Prager, J. S. Sarff, and D. Sinitsyn, Phys. Plasmas **4**, 1632 (1997).

[9] R. Bartiromo, P. Martin, S. Martini, T. Bolzonella, A. Canton, P. Innocente, L. Marrelli, A. Murari, and R. Pasqualotto, Phys. Rev. Lett. **82**, 1462 (1999).

[10] B. E. Chapman, A. F. Almagri, J. K. Anderson, C.-S. Chiang, D. Craig, G. Fiksel, N. E. Lanier, S. C. Prager, J. S. Sarff, M. R. Stoneking, and P. W. Terry, Phys. Plasmas **5**, 1848 (1998).

[11] N. E. Lanier, D. Craig, J. K. Anderson, T. M. Biewer, B. E. Chapman, C. B. Forest, S. C. Prager, D. L. Brower, and Y. Jiang, Phys. Rev. Lett. (to be published).

[12] G. Fiksel, D. J. Den Hartog, and P. W. Fontana, Rev. Sci. Instrum. **69**, 2024 (1998).

[13] D. J. Den Hartog and R. J. Fonck, Rev. Sci. Instrum. **65**, 3238 (1994).

[14] B. E. Chapman, Ph.D. thesis, University of Wisconsin-Madison, Madison, 1997.

[15] C. R. Sovinec, Ph.D. thesis, University of Wisconsin-Madison, Madison, 1995.

[16] C. R. Sovinec and S. C. Prager, Nucl. Fusion **39**, 777 (1999).